nature nanotechnology

SUPPLEMENTARY INFORMATION

DOI: 10.1038/NNANO.2014.182

Sensitive room-temperature terahertz detection via the photothermoelectric effect in graphene

Xinghan Cai[1], Andrei B. Sushkov[1], Ryan J. Suess[2], Mohammad M. Jadidi[2], Gregory S. Jenkins[1], Luke O. Nyakiti[4], Rachael L. Myers-Ward[5], Shanshan Li[2], Jun Yan[1,6], D. Kurt Gaskill[5], Thomas E. Murphy[2], H. Dennis Drew[1], Michael S. Fuhrer[1,3]

[1]Center for Nanophysics and Advanced Materials, University of Maryland, College Park, MD 20742-4111 USA; [2]Institute for Research in Electronics and Applied Physics, University of Maryland, College Park, MD 20742 USA; [3]School of Physics, Monash University, 3800 Victoria, Australia; [4]Texas A&M University, Galveston, TX 77553; [5]U.S. Naval Research Laboratory, Washington, DC 20375, USA; [6]Department of Physics, University of Massachusetts, Amherst, MA 01003, USA

Supplementary Notes

Supplementary Note 1: Raman spectroscopy of graphene

We performed Raman spectroscopy on our exfoliated graphene used for the device shown in Fig. 1f and SiC graphene used for the device shown in Fig. 4b inset of the main text. The spectra are shown in Supplementary Fig. 1 (a)- (c).The single-Lorentzian 2D peak indicates single layer graphene in both cases and the near absence of the D peak in Supplementary Fig. 1 (a) shows that our exfoliated graphene's quality is high.

Supplementary Note 2: Power dependence

Since both the electron thermal conductivity and the Seebeck coefficient of graphene are proportional to the temperature according to the Wiedemann-Franz law and Mott relation, the thermal voltage, either generated by Joule heating or photon excitation, should be linearly dependent on the absorbed power. Supplementary Fig. 2 shows the power dependence of the response for Joule heating, near-IR and far-IR radiation at a fixed gate voltage. The data is taken on one device for Supplementary Fig. 2(a-b) and on another similar device for Supplementary Fig. 2(c). Red lines are linear fitting to the experimental result. Supplementary Fig. 2 shows that the voltage response is proportional to the absorbed power (i.e. the responsivity is independent of power) over a power variation of 3 orders of magnitude. We also measured gate-voltage dependent responsivity of the device at various applied powers and find the linear response happens at all gate voltages, verifying that the device is operating in the linear regime at room temperature, and that our assumption that the signal is generated by heating is correct.

Supplementary Note 3: Absorbed power calculation

In order to quantitatively analyze the responsivity of the device in the main text, we consider the responsivity to absorbed power instead of the total incident power. Here we show how we calculate the absorbed power of the device which shows a peak responsivity of 715 V/W. We first measured the power intensity distribution of the laser beam. Since our device's active area is much smaller than the laser's spot size, we can approximate the device as a point. As shown in Supplementary Fig. 3, when scanning the beam across the device, the spatial distribution of the photovoltage signal reflects the beam intensity profile. We fit the data using a Gaussian function:

$$V_{photo} = V_{bg} + \frac{V_0}{w\sqrt{\pi/2}} e^{-2r^2/w^2}$$

where V_{bg} is the background signal due to electrical pick-up and other noise source and r is the distance to the center of the device. As shown in the inset of Supplementary Fig. 3, the graphene flake's size is ~ 2.0 μm x 2.1 μm. For convenience of calculation, we approximate its shape as a disk with the same area (radius $\mathrm{r_0} = 1.16\ \mu\mathrm{m}$). Considering the total incident power of 17 mW (The laser power was measured with a thermopile calibrated at NIST, Boulder.), the power on device's active area can be expressed as:

$$\mathrm{P_{active}} = \mathrm{P_0} \cdot \frac{\int_0^{\mathrm{r_0}} \mathrm{e}^{-2\mathrm{r}^2/\mathrm{w}^2}\mathrm{rdr}}{\int_0^{\infty} \mathrm{e}^{-2\mathrm{r}^2/\mathrm{w}^2}\mathrm{rdr}} = 0.75\ \mu\mathrm{W}$$

In addition, monolayer graphene will absorb only a small fraction of the incident power. In the THz range, the absorption is mainly due to the Drude response and can be expressed as $\mathrm{P} = \frac{1}{2}\mathrm{Re}[\sigma(\omega)]|\mathrm{E_t}|^2\mathrm{A}$, where $\sigma(\omega)$ is graphene's conductivity, $\mathrm{E_t}$ is the electric field on the graphene of area A. The electric field on graphene is related with the electric field of the incident beam $\mathrm{E_0}$ as $\mathrm{E_t} = \frac{2\mathrm{E_0}}{|1+\mathrm{n}+\mathrm{Z_0}\sigma(\omega)|}$, where n = 3.42 is the refractive index of silicon substrate and $\mathrm{Z_0} = 377\Omega$ is the impedance of free space. Using the equation of the incident light intensity $\mathrm{I_0} = \frac{\mathrm{E_0^2}}{2\mathrm{Z_0}}$, we can write the absorption rate of graphene as:

$$\eta = \frac{\mathrm{P}}{\mathrm{P_0}} = \frac{\mathrm{Re}[\sigma(\omega)]|\mathrm{E_t}|^2/2}{\mathrm{E_0^2}/2\mathrm{Z_0}} = \frac{4\mathrm{Z_0}\mathrm{Re}[\sigma(\omega)]}{|1+\mathrm{n}+\mathrm{Z_0}\sigma(\omega)|^2}$$

For our wavelength $\lambda = 119\ \mu\mathrm{m}$, $\sigma(\omega)$ can be approximated as our measured dc conductivity σ_0. Taking into account that our maximum photovoltage signal is 8.1μV, the peak responsivity is then expressed as:

$$\mathrm{Responsivity^{max}} = \frac{\mathrm{V_{photo}^{max}}}{\mathrm{P_{active}} \cdot \eta} = 715\mathrm{V/W}$$

Supplementary Note 4: Device response modelling

Modeling the device response was done as follows. The device was approximated as a 3 μm × 3 μm square. We assume that the local electrical conductivity σ of graphene depends on the local Fermi energy E_F as:

$$\sigma = \sigma_{\min}(1+\frac{E_F{}^4}{\Delta^4})^{1/2} \quad \text{(S1)}$$

where σ_{min} is the minimum conductivity and Δ is a parameter that expresses the disorder strength[S1]. This functional form for σ correctly extrapolates between the highly doped region where σ ~ E_F^2 and the charge neutral point where σ ~ constant. Supplementary Figure 4 reproduces the *G*(*Vg*) data from Fig. 2a with a fit to Eqn. S1 (red curve) to obtain σ_{min} = 0.169 mS and Δ =107 meV. To treat asymmetry in contact metal we followed the results of reference [S2] to obtain the charge carrier distribution across the device and thus the local Fermi level. Then we numerically solve the 1D diffusive heat conductance equation to get the temperature profile across the device[S1]. Given the temperature profile and local Fermi level we calculate the thermoelectric field $E = S\nabla T$, where S is given by Eqn. (S1) and the Mott relation $S = LT(d\ln\sigma/dE_F)$, and integrate over the device to obtain the thermoelectric voltage. For chromium and gold we select parameters V_{b1} = 65 meV and V_{b2} = 265 meV for gold, V_{b1} = -67 meV and V_{b2} = 65 meV for chromium according to the model in Reference[S2].

We treat the thermoelectric signal due to asymmetric contact resistance as follows. We assume that the whole device is uniformly doped with Fermi energy determined by the gate voltage, and add an extra contact resistance R_c = 33.5 Ω to the region from the gold contact extending 100 nm inside the graphene (the corresponding contact resistivity is ρ_c = 1000 Ω). Then, the conductivity of this region can be rewritten as

$$\frac{1}{\sigma} = \frac{1}{\sigma_{\min}(1+\frac{E_F{}^4}{\Delta^4})^{1/2}} + \rho_c .$$

The electron thermal conductivity and Seebeck coefficient in this region change correspondingly.

To model the combined effects of contact metal and contact resistance, we first calculate the Fermi level distribution taking into account the contact metal asymmetry. The temperature profile is calculated from the thermal conductivity assuming an extra contact resistance R_c = 33.5 Ω in the region from the gold contact extending 100 nm inside the graphene. The local Seebeck coefficient and the thermopower are then calculated as before.

References

[S1] Song, J.C.W., Rudner, M.S., Marcus C.M. & Levitov, L.S. Hot carrier transport and photocurrent response in graphene. *Nano Lett.* **11**, 4688-4692 (2011)

[S2] Khomyakov, P.A., Starikov, A.A., Brocks, G. & Kelly, P.J. Nonlinear screening of charges induced in graphene by metal contacts. *Phys. Rev. B* **82**, 115437 (2010)

Supplementary Figures

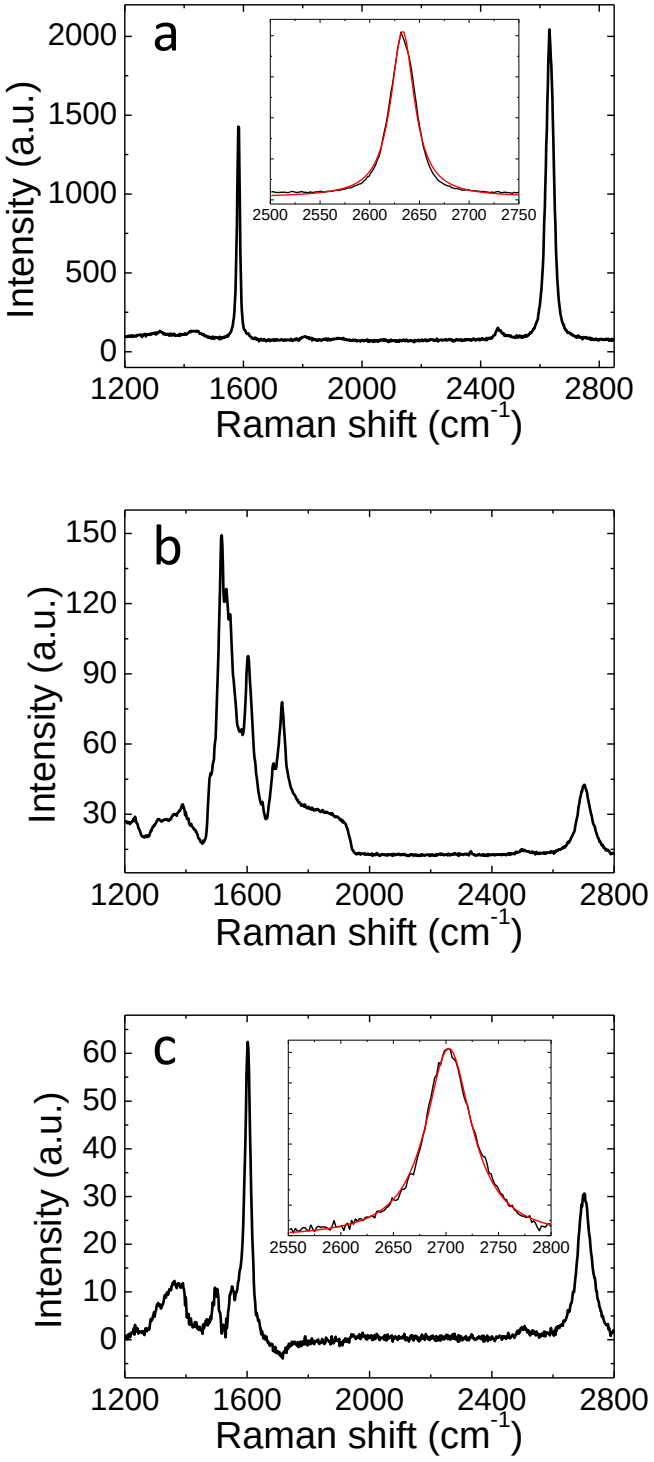

Supplementary Fig. 1 Raman spectrum of graphene used for device shown (a) in Fig. 1f, main text (b) in Fig. 4b inset, main text (c) in Fig. 4b inset, main text (SiC background spectrum subtracted). The inset of (a) and (c) shows a Lorentzian fit (red line) to the 2D peak (black line) of corresponding spectrum.

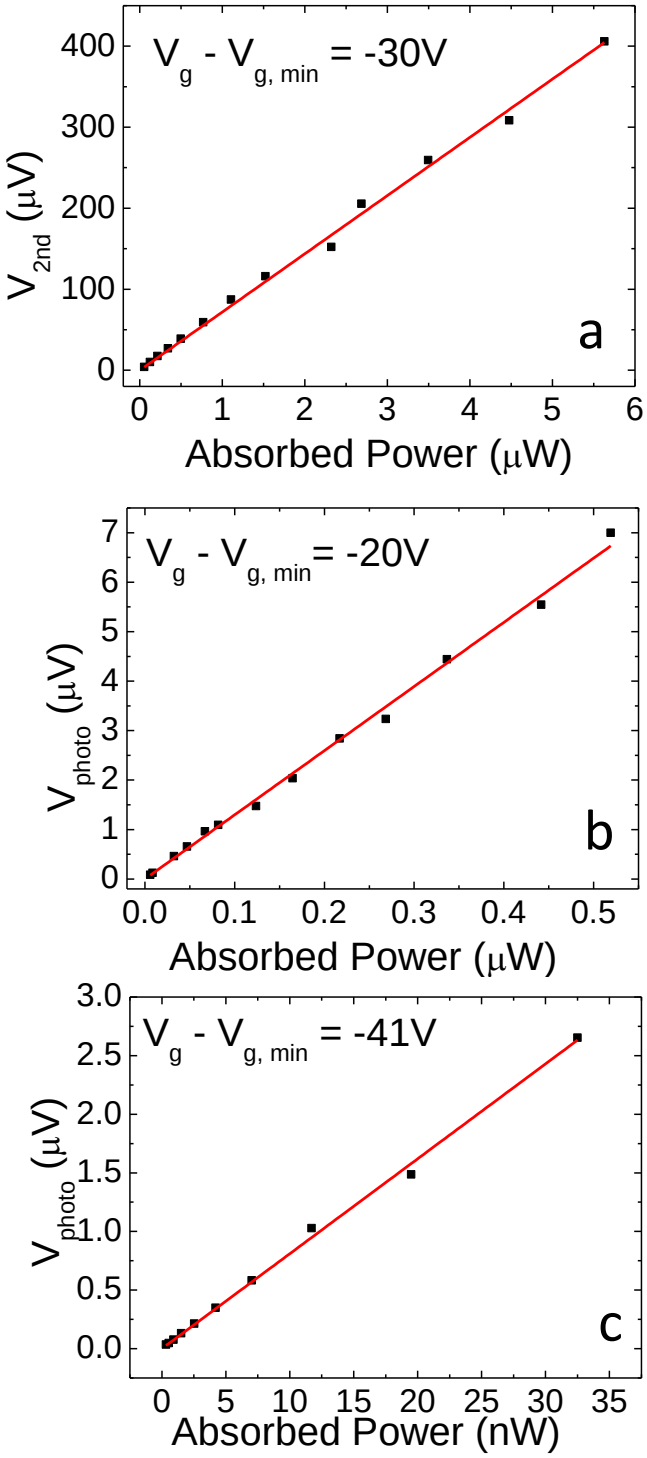

Supplementary Fig. 2 Voltage signal as a function of applied power for (a) ac Joule heating at $V_g - V_{g,min}$ = -30 V, (b) 1.54 μm near infrared radiation at $V_g - V_{g,min}$ = -20V and (c) 119 μm far infrared radiation at $V_g - V_{g,min}$ = -41V.

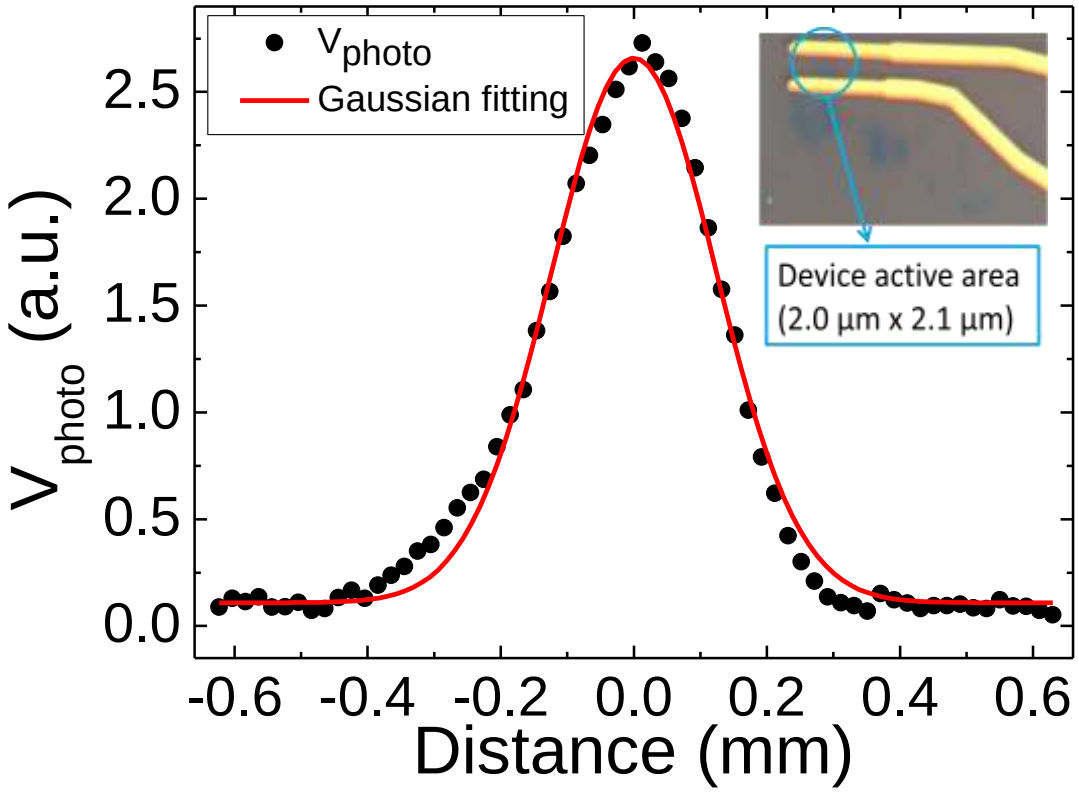

Supplementary Fig. 3 Photovoltage for the graphene photothermoelectric detector as a function of distance measured as the far infrared laser is scanned across the device (black dots) and Gaussian fit to the experimental data (red curve). Inset: Optical micrograph of the device. The device active area (graphene flake) is between two metal electrodes.

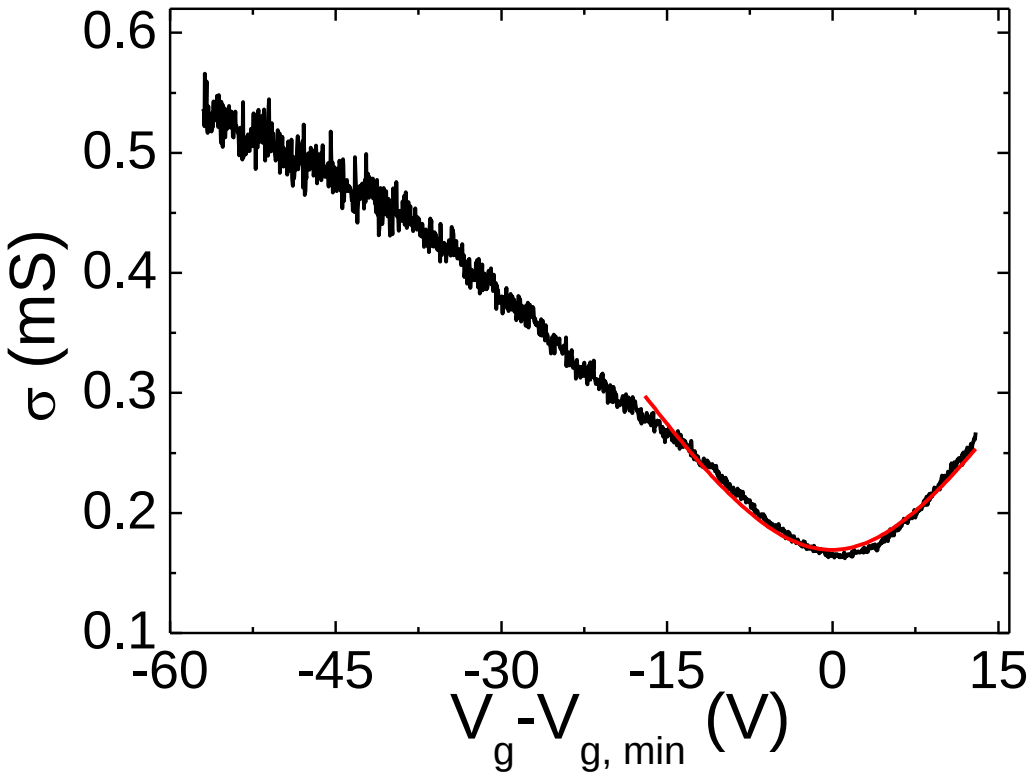

Supplementary Fig. 4 Electrical conductance as a function of gate voltage (black curve) for the device shown in Fig. 1f. Red solid line is a fit to Eqn. S1.